Reactive & Functional Polymers 91–92 (2015) 85–92

Contents lists available at ScienceDirect

Reactive & Functional Polymers

journal homepage: www.elsevier.com/locate/react

Controlled synthesis of photosensitive graft copolymers with high azobenzene-chromophore loading densities in the main and side chains by combining ATRP and ADMET polymerization

Liang Ding [a,*], Juan Li [a], Chengshuang Wang [a], Ling Lin [a,b]

[a] School of Materials Engineering, Yancheng Institute of Technology, Yancheng 224051, China
[b] Key Laboratory of Eco-Textile, Ministry of Education, Jiangnan University, Wuxi 214122, China

ARTICLE INFO

Article history:
Received 25 March 2015
Received in revised form 2 May 2015
Accepted 7 May 2015
Available online 14 May 2015

Keywords:
Graft copolymer
Azobenzene
Main–side chains
ATRP
ADMET polymerization

ABSTRACT

Photosensitive graft copolymers containing azobenzene chromophores in the main and side chains were successfully synthesized by combining living atom transfer radical polymerization (ATRP) and acyclic diene metathesis (ADMET) chemistry based on the results of proper heterodifunctional inimer and azobenzene monomer design. The precise copolymer architectural features were manipulated by combining the macromonomer technique and the macroinitiator method. The as-prepared copolymer containing azobenzene chromophores in the main and side chains showed unique reversible isomerization processes, suggesting that the photoisomerization of azobenzene chromophores occured mainly in one of the two types of azobenzene groups in the main or side chains with similar probabilities due to their main and side-on structure.

1. Introduction

Polymers containing azobenzene chromophores have received significant attention because of their two unique properties: photoinduced reversible *trans–cis* isomerization and nonlinear optical properties [1,2]. Generally, azobenzene-containing polymers (azo polymers) can be divided into main-chain and side-chain types according to the locations of the azo groups in the polymers [3,4]. These two polymer types have some distinct differences in their thermal stabilities [5] and chain anisotropies [6]. Polymers containing azo group in the main and side chains can be easily prepared by either random copolymerization of azo monomers without reactive groups with another monomer with a reactive group [7,8] or direct living polymerization of azo monomers with reactive groups [9,10]. However, most investigations have focused on the incorporation of azo groups into either the main chains or the side chains, and there are few reports on polymers with azo chromophores in both the main and side chains, most likely due to the rather limited synthetic methods. Based on the above statements, it can be concluded that, despite the fact that the synthesis of main and side chain, azo polymers remains a challenge, they have a promising future in many applications. Therefore, the development of new main and side chain azo-functionalized polymers is important.

Graft copolymers are regularly branched macromolecules consisting of a backbone, and many side chains [11]. They offer unique material properties that can be tailored by changing the polymer backbone and the graft chains [12]. The design of controlled graft copolymers through various methods has become the focus of interesting research in which the physical and chemical properties can be purposely altered by combining different polymer components in an ordered fashion [13]. Generally, well-defined graft copolymers with various architectures have been synthesized using multiple controlled/living polymerization methods [14]. Among these diverse polymerization strategies, metathesis polymerization and radical polymerization are particularly suitable for the preparation of graft copolymers due to the controlled molecular weight, relatively narrow molecular weight distribution, and desired topology of the resulting polymers [15–19].

Olefin metathesis-based step-growth polymerization, called acyclic diene metathesis (ADMET) polymerization, is performed with α,ω-dienes and proceeds via the release of ethylene as a condensate [20,21]. It is well known that ADMET polymerization successfully yields unsaturated, linear, and high molecular weight polymers possessing various functional groups, both within and pendant to them [22]. This approach has led to a wide range of unsaturated and saturated polymers bearing different

* Corresponding author. Tel.: +86 515 88298872.
E-mail address: dl1984911@ycit.edu.cn (L. Ding).

http://dx.doi.org/10.1016/j.reactfunctpolym.2015.05.003
1381-5148/

functionalities with the possibility of modifying the polyolefin architectures by placing precise functional groups throughout the backbone [23]. Wagener explored this polymerization technique and prepared a new type of graft copolymer by combining atom transfer radical polymerization (ATRP) and ADMET polymerization [24]. These methods provide the possibility of preparing azo-containing main–side chain graft copolymers. However, to the best of our knowledge, up to now, only three classes of metathesis azo-polymer based on more defined polymeric structures (linear, hyperbranched and long-chain highly branched polymers) have been reported by our group [25].

Consequently, the goal in this research is to exploit the ADMET polymerization scheme for the preparation of densely grafted molecular brushes with azo units in the main and side chains. According to "Route 1", the azo-functionalized α,ω-diene inimer **4** first initiated ATRP of the as-prepared azo monomer **M1** using CuBr/PMDETA as a catalyst and ligand, yielding a macromonomer in the subsequent ADMET polymerization. The second route relies upon ADMET polymerization of inimer **4** catalyzed by a Grubbs third generation catalyst (**Ru-III**) to produce a macroinitiator followed by initiating ATRP of **M1** (Scheme 1).

2. Experimental

2.1. Materials

Methacrylic acid (99%), 10-undecenoic acid (99%), 2-bromoethanol (98%), 3-mercapto-1,2-propanediol (90%), 2-bromoisobutyryl bromide (97%), dichloro[1,3-bis(2,4,6-trimethyl phenyl)-2-imidazolidinylidene](benzylidene)bis(3-bromopyridine) ruthenium (II) (Grubbs third generation catalyst, **Ru-III**), 1-[3-(di methylamino)propyl]-3-ethylcarbodiimide hydrochloride (EDCI·HCl, >99%), and N,N,N′,N″,N″-pentamethyldiethylenetriamine (PMDETA, 98%) were purchased from Energy Chemical (Shanghai) and used as received, without purification. The solvents were distilled over drying agents under nitrogen prior to use. Copper(I) bromide (CuBr, Alfa Aesar, 97%) was purified by washing with glacial acetic acid, followed by ethanol and ethyl ether, and then dried under vacuum. Triethylamine (Et_3N) and pyridine were freshly distilled and dried. The azobenzene functional asymmetric α,ω-diene monomer (**M2**) was synthesized as reported previously by our group [25c].

2.2. Characterization

ATR–IR spectra were recorded on a Bruker Tensor 37 in the region of 4000–400 cm^{-1} using attenuated total reflection (ATR). UV–vis absorption spectra were measured on a Cary 60 spectrometer. UV irradiation was performed using an 8-W UV lamp with a wavelength of 365 nm. Irradiation by visible light was performed using a 23-W Philips day light bulb (>400 nm). Elemental analysis (EA) was conducted using an Elementar Vario EL. Gas chromatography (GC) was measured using an Agilent 6890 series GC system instrument equipped with a flame ionization detector and a capillary column (HP–5. 0.25 mm × 30 m), using decane as an internal standard; T_{inj} 280 °C, T_{detec} 280 °C, T_{init} 50 °C (10 °C/min), carrier gas: N_2. High–resolution mass spectrometry (HRMS) data were recorded on a Waters GCT Premier mass spectrometer in electron ionization mode. LC/MS measurements were performed using an Agilent technology 1200 series at 45 °C using H_2O or CH_3CN as the mobile phase on a 50 m × 4.6 mm × 3.5 μm diffused column. ^1H (500 MHz) and ^{13}C (125 MHz) NMR spectra were recorded using tetramethylsilane as an internal standard in $CDCl_3$ on a Bruker DPX spectrometer. Multiangle laser light scattering–gel permeation chromatography (MALLS–GPC) was employed to evaluate the molecular weights of the synthesized samples. The MALLS–GPC system consisted of a Waters 2690D Alliance liquid chromatography system, a Wyatt Optilab DSP differential refractometer detector (690 nm, Wyatt Technology), and a Wyatt DAWN EOS MALLS detector (30 mW GaAs linearly polarized laser, 690 nm). Two chromatographic columns (Styragel HR3, HR4) with a precolumn were used in series. THF was used as the mobile phase at a flow rate of 1.0 mL/min at 30 °C. A 100-μL sample of a 3.0 mg/mL solution, which was filtered through a 0.2-μm Whatman filter prior to use, was injected for all measurements. The increase in the refractive index (dn/dc) of the polymer samples in THF was determined using a Wyatt Optilab DSP differential refractometer at 690 nm. The data analysis was performed using Astra software (ver. 4.90.04, Wyatt Technology).

Polymerizations were performed in Schlenk tubes using a nitrogen flow to drive off the ethylene condensate during ADMET.

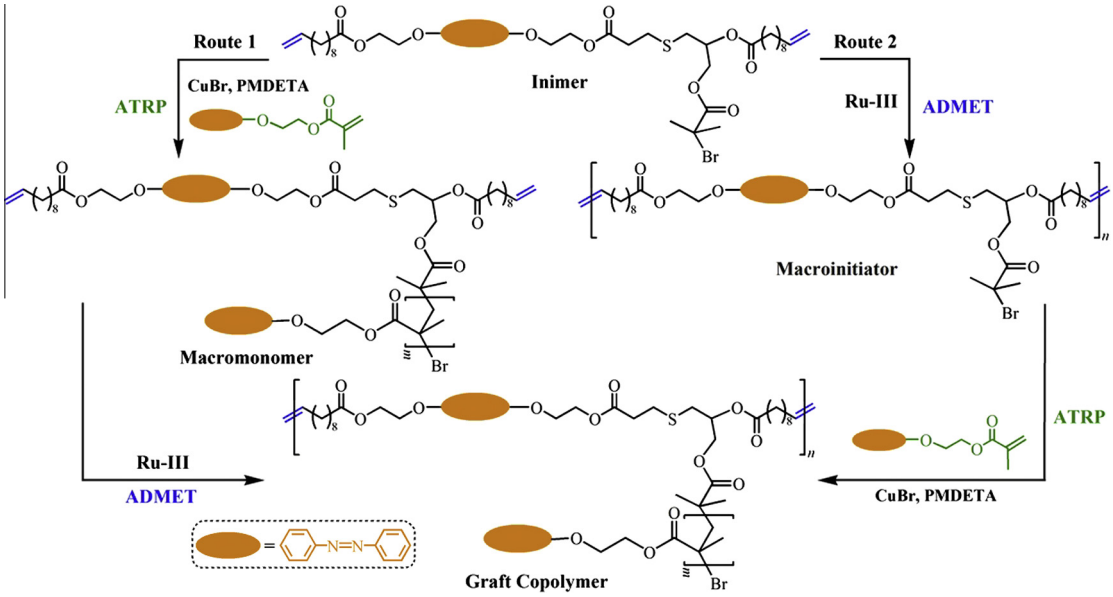

Scheme 1. Synthetic routes to azobenzene functionalized graft copolymers via commutative combination of ATRP and ADMET polymerization.

2.3. Synthesis of methacrylic acid 2-bromo-ethyl ester (**1**)

Methacrylic acid (4.30 g, 50 mmol), 2-bromoethanol (9.38 g, 75 mmol), and DMAP (0.75 g, 6 mmol) were added to a Schlenk flask and dissolved in 100 mL of dried CH_2Cl_2 under a nitrogen atmosphere. Then, EDCI (11.48 g, 60 mmol) was added at 0 °C with rapid stirring. The reaction mixture was allowed to warm to room temperature and stirred for an additional amount of time. After 3 days, the resulting solution was subsequently washed with 1 M HCl, saturated $NaHCO_3$ aq., and deionized water. The organic layer was separated and dried over anhydrous Na_2SO_4. Then, it was evaporated to afford a yellowish liquid (8.36 g, 86.6% yield). ^{1}H NMR (500 MHz, $CDCl_3$, δ): 6.51–6.43 (m, 1H, C*H*═CCH$_3$COO), 5.97–5.82 (m, 1H, C*H*═CCH$_3$COO), 4.42–4.17 (m, 2H, C*H*$_2$CH$_2$Br), 3.61–4.30 (m, 2H, CH$_2$C*H*$_2$Br), 2.09–1.73 (m, 3H, CH═CC*H*$_3$COO). ^{13}C NMR (125 MHz, $CDCl_3$, δ): 165.6, 139.1, 123.3, 71.7, 33.1, 18.5. GC: single peak was observed. EI/HRMS: Calcd. for $C_6H_9O_2Br$: 193.0427; found: 193.0326. Anal. calcd. for $C_6H_9O_2Br$: C 37.33, H 4.70, O 16.58; Found: C 37.46, H 4.45, O 16.57.

2.4. Synthesis of 4-(2-ethyoxy methacrylate) azobenzene (***M1***)

4-Hydroxy azobenzene (5.94 g, 30 mmol), potassium carbonate (16.56 g, 120 mmol), and 90 mL of DMF were charged into a 250-mL Schlenk flask. The reaction mixture was heated at 80 °C for 6 h under nitrogen, thus allowing the potassium salt to form. A solution of compound **1** (6.95 g, 36 mmol) in 30 mL of DMF was then added dropwise to the above mixture. After 24 h of stirring at 50 °C, the reaction mixture was poured into 1 L of deionized water and the crude product precipitated. This product was further purified by recrystallization from ethanol to give a red crystal (7.55 g, 81.2% yield). ^{1}H NMR (500 MHz, $CDCl_3$, δ): 8.08–7.96 (m, 4H, *o*-Ar*H*—N═N—Ar*H*), 7.56–7.49 (m, 3H, *m*-Ar*H*—N═N—ArH + *p*-Ar*H*—N═N—ArH), 7.02–6.93 (d, 2H, *m*-ArH—N═N—Ar*H*), 6.22–6.17 (m, 1H, C*H*═CCH$_3$COO), 5.87–5.81 (m, 1H, C*H*═CCH$_3$COO), 4.62–4.49 (m, 2H, CH$_2$═CCH$_3$COOC*H*$_2$CH$_2$), 4.36–4.27 (m, 2H, CH$_2$═CCH$_3$COOCH$_2$C*H*$_2$), 1.95–1.89 (m, 3H, CH═CC*H*$_3$COO). ^{13}C NMR (125 MHz, $CDCl_3$, δ): 165.8, 161.3, 153.5, 144.7, 136.9, 131.0, 128.2, 123.3, 122.8, 115.1, 73.5, 67.6, 18.2. LC: single peak was observed. EI/MS: Calcd. for $C_{18}H_{18}O_3N_2$: 310.34; found: 310.32. Anal. calcd. for $C_{18}H_{18}O_3N_2$: C 69.64, H 5.85, O 15.45; Found: C 69.66, H 5.85, O 15.47.

2.5. Synthesis of the dihydroxyl azobenzene compound (***2***)

M2 (5.23 g, 10 mmol), 3-mercapto-1,2-propanediol (1.62 g, 15 mmol), Et_3N (2.02 g, 20 mmol) and THF (50 mL) were charged into a round-bottom flask equipped with a magnetic stirrer under nitrogen atmosphere, and the mixture was stirred overnight at room temperature. The resulting solution was concentrated and precipitated into excess deionized water. The product precipitated and dried under vacuum to give a red solid (5.62 g, 89.1% yield). ^{1}H NMR (500 MHz, $CDCl_3$, δ): 7.97–7.86 (m, 4H, *o*-Ar*H*—N═N—Ar*H*), 7.01–6.89 (m, 4H, *m*-ArH—N═N—Ar*H*), 5.82–5.76 (d, 1H, CH$_2$═C*H*), 5.06–4.95 (m, 2H, C*H*$_2$═CH), 4.51–4.42 (m, 2H, CH$_2$C*H*$_2$OCO), 4.26–4.03 (m, 2H, C*H*$_2$CH$_2$OCO), 3.61–3.52 (m, 3H, C*H*OHC*H*$_2$OH), 2.73–2.50 (m, 6H, C*H*$_2$C*H*$_2$SC*H*$_2$), 2.20–2.13 (m, 2H, OCOC*H*$_2$), 2.04–1.98 (m, 2H, CH$_2$═CHC*H*$_2$), 1.90–1.69 (m, 2H, OCOCH$_2$C*H*$_2$), 1.47–1.06 (m, 12H, C*H*$_2$). ^{13}C NMR (125 MHz, $CDCl_3$, δ): 171.8, 161.3, 144.7, 139.6, 123.3, 115.2, 76.5, 71.6, 68.1, 66.7, 36.8, 34.2, 29.4, 27.6, 23.2. LC: single peak was observed. EI/MS: Calcd. for $C_{33}H_{46}O_8N_2S$: 630.79; found: 630.74. Anal. calcd. for $C_{33}H_{46}O_8N_2S$: C 62.83, H 7.35, O 20.29; Found: C 62.80 H 7.35, O 20.27.

2.6. Synthesis of the hydroxyl bromoisobutyryloxy azobenzene compound (***3***)

Compound **2** (5.05 g, 8 mmol) was dissolved in 30 mL of THF, and dry Et_3N (2.42 g, 24 mmol) was added under nitrogen. The reaction mixture was cooled to 0 °C before 2-bromoisobutyryl bromide (0.9 mL, 7.2 mmol) was added dropwise to this solution via syringe. The reaction mixture was then warmed to room temperature and stirred for another 24 h. During this time, a white precipitate formed. The precipitate was filtered off, and the filtrate was subsequently concentrated and precipitated in excess deionized water. The crude product precipitated and was further purified using silica gel chromatography eluted with methylene chloride/methanol (50/1, R_f = 0.5) to afford a red solid (4.41 g, 70.6% yield). ^{1}H NMR (500 MHz, $CDCl_3$, δ): 7.98–7.89 (m, 4H, *o*-Ar*H*—N═N—Ar*H*), 7.02–6.87 (m, 4H, *m*-ArH—N═N—Ar*H*), 5.84–5.77 (d, 1H, CH$_2$═C*H*), 5.03–4.96 (m, 2H, C*H*$_2$═CH), 4.55–4.47 (m, 2H, CH$_2$C*H*$_2$OCO), 4.24–4.02 (m, 3H, C*H*$_2$CH$_2$OCO + C*H*OCOCH$_2$OH), 3.72–3.59 (m, 2H, CHOCOC*H*$_2$OH), 2.77–2.53 (m, 6H, C*H*$_2$C*H*$_2$SC*H*$_2$), 2.22–2.10 (m, 2H, OCOC*H*$_2$), 2.06–1.93 (m, 8H, CH$_2$═CHC*H*$_2$ + OCOCC*H*$_3$BrC*H*$_3$), 1.79–1.62 (m, 2H, OCOCH$_2$C*H*$_2$), 1.42–1.11 (m, 12H, C*H*$_2$). ^{13}C NMR (125 MHz, $CDCl_3$, δ): 176.2, 172.1, 161.7, 144.2, 140.3, 123.6, 114.5, 80.6, 72.2, 67.7, 66.0, 52.1, 35.5, 33.7, 29.8, 27.9, 25.3, 24.1. LC: single peak was observed. EI/MS: Calcd. for $C_{37}H_{51}O_9N_2SBr$: 779.77; found: 779.79. Anal. calcd. for $C_{37}H_{51}O_9N_2SBr$: C 56.99, H 6.59, O 18.47; Found: C 57.01, H 6.56, O 18.47.

2.7. Synthesis of the azobenzene-containing α,ω-diene inimer (***4***)

Compound **3** (3.90 g, 5 mmol), 10-undecenoic acid (1.11 g, 6 mmol), DMAP (0.08 g, 0.6 mmol), CH_2Cl_2 (22 mL), and THF (8 mL) were charged into a 100-mL round-bottom flask equipped with a magnetic stirrer under a nitrogen atmosphere, and the mixture was stirred at 0 °C for 15 min. EDCI (1.12 g, 6 mmol) was then added to the former solution, which was stirred for 3 days after the solution warmed to room temperature. The resulting solution was washed three times with deionized water (3 × 80 mL), and the organic layer was dried over anhydrous Na_2SO_4. The solvent was then evaporated and the crude product was purified by silica gel chromatography eluted with methylene chloride/petroleum ether (10/1, R_f = 0.6) to give a dark red solid (3.58 g, 75.7% yield). ^{1}H NMR (500 MHz, $CDCl_3$, δ): 8.04–7.76 (m, 4H, *o*-Ar*H*—N═N—Ar*H*), 7.05–6.83 (m, 4H, *m*-ArH—N═N—Ar*H*), 5.85–5.72 (d, 1H, CH$_2$═C*H*), 5.02–4.94 (m, 2H, C*H*$_2$═CH), 4.90–4.72 (CH$_2$C*H*OCOCH$_2$OCO), 4.53–4.46 (m, 2H, CH$_2$C*H*$_2$OCO), 4.37–4.07 (m, 4H, C*H*$_2$CH$_2$OCO + CH$_2$CHOCOC*H*$_2$OCO), 2.73–2.50 (m, 6H, C*H*$_2$C*H*$_2$SC*H*$_2$), 2.32–2.11 (m, 4H, OCOC*H*$_2$), 2.08–1.79 (m, 10H, CH$_2$═CHC*H*$_2$ + OCOCC*H*$_3$BrC*H*$_3$), 1.71–1.52 (m, 4H, OCOCH$_2$C*H*$_2$), 1.50–1.16 (m, 24H, C*H*$_2$). ^{13}C NMR (125 MHz, $CDCl_3$, δ): 175.6, 172.0, 161.4, 145.0, 139.7, 122.9, 115.2, 77.1, 72.8, 69.3, 66.4, 53.2, 36.5, 33.6, 29.9, 28.5, 26.8, 25.2. LC: single peak was observed. EI/MS: Calcd. for $C_{48}H_{69}O_{10}N_2SBr$: 946.02; found: 945.99. Anal. calcd. for $C_{48}H_{69}O_{10}N_2SBr$: C 60.94, H 7.35, O 16.91; Found: C 60.91, H 7.36, O 16.87.

2.8. ATRP for preparing macromonomer (First Step in Route 1)

A mixture of inimer (945 mg, 1 mmol), **M1** (4.65 g, 15 mmol), CuBr (288 mg, 2 mmol), PMDETA (420 μL, 2 mmol), 10 mL of THF, and 2 mL of CH_3OH was degassed by three freeze–vacuum–thaw cycles and then heated at 60 °C for 12 h under vacuum. The mixture was diluted in 20 mL of THF followed by passing through a column of basic alumina. The purified polymer was precipitated in excess methanol and then dried under vacuum for 24 h to give the macromonomer with a monomer conversion of 92%. ^{1}H NMR

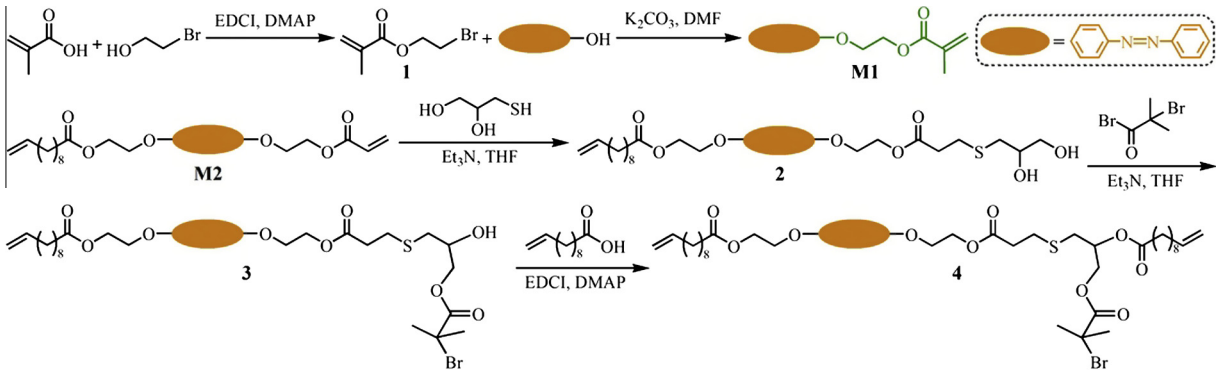

Scheme 2. General protocols for the preparation of the azobenzene functional inimer for ATRP.

(500 MHz, $CDCl_3$, δ): 7.95–7.67 (m, *o*-Ar*H*—N=N—Ar*H*), 7.58–7.29 (m, *p*-Ar*H*—N=N—ArH), 7.01–6.78 (m, *m*-Ar*H*—N=N—Ar*H*), 5.89–5.75 (d, CH_2=C*H*), 5.03–4.79 (m, CH_2=CH + $CH_2CHOCOCH_2OCO$), 4.52–4.43 (m, CH_2CH_2OCO), 4.27–4.02 (m, CH_2CH_2OCO + $CH_2CHOCOCH_2OCO$), 2.76–2.44 (m, $CH_2CH_2SCH_2$ + $OCOCH_2$), 2.12–1.77 (m, CH_2=$CHCH_2$ + CH_2CBrCH_3), 1.71–1.52 (m, CH_2 + $OCOCCH_3CH_3$). MALLS–GPC: M_n = 5300, M_w/M_n = 1.07; NMR: M_n = 5200.

2.9. Typical ADMET polymerization procedure for the synthesis of the azo-containing main–side chains graft copolymer (Second Step in Route 1)

In a nitrogen-filled Schlenk tube, a solution of **Ru-III** (0.5 mol% to macromonomer) in 0.2 mL of toluene degassed with three freeze–vacuum–thaw cycles was added to a solution of the macromonomer (0.5 mmol) in 0.8 mL of toluene degassed with the same procedure. After the reaction mixture was stirred at 60 °C for 24–96 h, the polymerization was quenched by adding ethyl vinyl ether with stirring for 30 min. The solution was precipitated in excess methanol, and the precipitate was isolated by filtration and dried under vacuum for 24 h to give the resulting graft copolymer as a dark red semisolid to solid. ^{1}H NMR (500 MHz, $CDCl_3$, δ): 8.05–7.78 (m, *o*-Ar*H*—N=N—Ar*H*), 7.61–7.28 (m, *p*-Ar*H*—N=N—ArH), 7.21–6.96 (m, *m*-Ar*H*—N=N—Ar*H*), 5.49–5.24 (d, C*H*=C*H*), 5.00–4.89 (s, $CH_2CHOCOCH_2OCO$), 4.68–4.47 (m, CH_2CH_2OCO), 4.31–3.99 (m, CH_2CH_2OCO + $CH_2CHOCOCH_2OCO$), 2.73–2.46 (m, $CH_2CH_2SCH_2$ + $OCOCH_2$), 2.22–2.10 (m, $OCOCH_2$), 2.07–1.81 (m, CH_2=$CHCH_2$ + CH_2CBrCH_3), 1.77–1.02 (m, CH_2 + $OCOCCH_3CH_3$). MALLS–GPC: M_n = 26,700, M_w/M_n = 2.23 for 24 h; M_n = 50,500, M_w/M_n = 2.08 for 48 h; M_n = 89,300, M_w/M_n = 1.89 for 72 h; M_n = 127,800, M_w/M_n = 1.92 for 96 h; NMR: M_n = 23,900 for 24 h; M_n = 84,200 for 72 h.

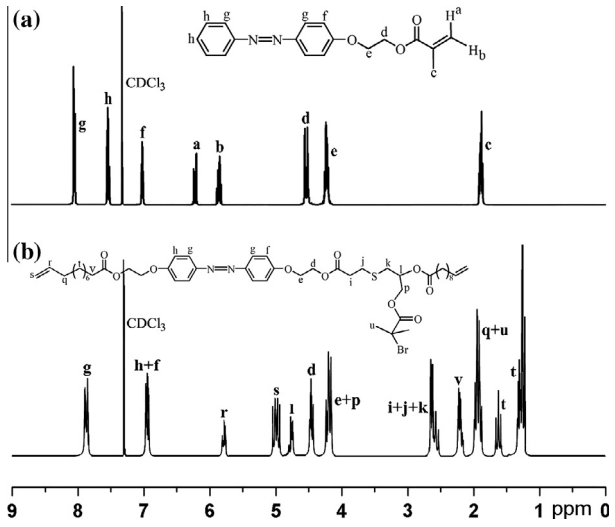

Fig. 1. ^{1}H NMR spectra for (a) ATRP monomer **M1** and (b) inimer **4**.

2.10. General ADMET polymerization procedure for the synthesis of the macroinitiator (First Step in Route 2)

In a nitrogen–filled Schlenk tube, a solution of **Ru-III** (0.5 mol% to inimer **4**) in toluene was degassed with three freeze–vacuum–thaw cycles and then added to a degassed (with the same procedure as above) solution of inimer **4** (0.5 mmol, 473 mg) in toluene. After stirring at 60 °C for 24 h, the polymerization was quenched by adding ethyl vinyl ether with stirring for 30 min. Then, the reaction mixture was precipitated in excess methanol, and the precipitate was isolated by filtration and dried under vacuum for 24 h to give the macroinitiator at high yields. ^{1}H NMR (500 MHz, $CDCl_3$, δ): 8.03–7.83 (m, *o*-Ar*H*—N=N—Ar*H*), 7.22–6.90 (m, *m*-Ar*H*—N=N—Ar*H*), 5.47–5.21 (d, C*H*=C*H*), 4.92–4.83 (s, $CH_2CHOCOCH_2OCO$), 4.61–4.43 (m, CH_2CH_2OCO), 4.28–3.96 (m, CH_2CH_2OCO + $CH_2CHOCOCH_2OCO$), 2.77–2.42 (m, $CH_2CH_2SCH_2$ + $OCOCH_2$), 2.25–2.11 (m, $OCOCH_2$), 2.06–1.78 (m, CH_2=$CHCH_2$ + $OCOCCH_3CH_3$), 1.76–1.20 (m, CH_2). MALLS–GPC: M_n = 18,300, M_w/M_n = 2.21; NMR: M_n = 17,500.

2.11. Representative procedure for the preparation of the azo-containing main–side chains graft copolymer via ATRP (Second Step in Route 2)

The macroinitiator produced by ADMET polymerization (0.02 mmol) in 1 mL of THF, **M1** (93 mg, 0.3 mmol), CuBr (14.4 mg, 0.1 mmol) and PMDETA (21 μL, 0.1 mmol) in 1 mL of THF and 0.5 mL of CH_3OH were charged into a Schlenk tube. After degassing of the mixture by three freeze–vacuum–thaw cycles, the tube was sealed under vacuum and then heated at 60 °C for 24 h. The reaction was quenched by removal of the heat and exposure to air. The mixture was diluted in 15 mL of THF and then passed through a short column of basic alumina to remove the copper residues. The purified copolymer was precipitated in petroleum ether twice, and then dried under vacuum for 24 h to give the resulting graft copolymer as a dark red solid with a monomer conversion of 20%. ^{1}H NMR (500 MHz, $CDCl_3$, δ): 8.05–7.78 (m, *o*-Ar*H*—N=N—Ar*H*), 7.61–7.28 (m, *p*-Ar*H*—N=N—ArH), 7.21–6.96 (m, *m*-Ar*H*—N=N—Ar*H*), 5.49–5.24 (d, C*H*=C*H*), 5.00–4.89 (s, $CH_2CHOCOCH_2OCO$), 4.68–4.47 (m, CH_2CH_2OCO), 4.31–3.99 (m, CH_2CH_2OCO + $CH_2CHOCOCH_2OCO$), 2.73–2.46 (m, $CH_2CH_2SCH_2$ + $OCOCH_2$), 2.22–2.10 (m, $OCOCH_2$), 2.07–1.81 (m,

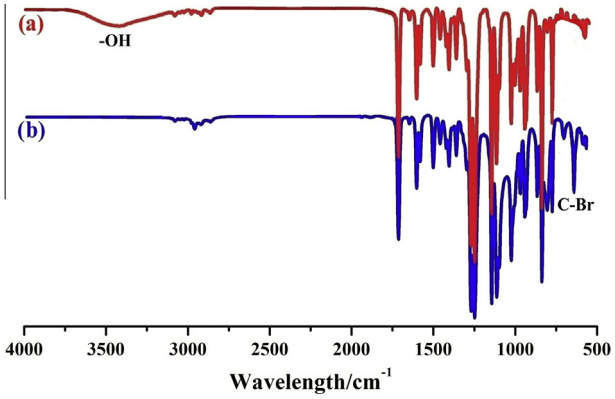

Fig. 2. ATR–IR spectra for (a) compound **2** and (b) inimer **4**.

CH_2=CHCH_2 + CH_2CBrCH_3), 1.77–1.02 (m, CH_2 + OCOC$CH_3$$CH_3$). MALLS–GPC: M_n = 35,500, M_w/M_n = 2.37; NMR: M_n = 36,800.

3. Results and discussion

3.1. Preparation of the ATRP monomer and inimer

The synthesis of 4-(2-ethyoxy methacrylate) azobenzene (**M1**), which is depicted in Scheme 2, involved the Williamson coupling reaction of the as-prepared methacrylic acid 2-bromo-ethyl ester (**1**) with 4-hydroxy azobenzene in high yield. ^{1}H NMR (Fig. 1a), LC/MS, and elemental analysis confirmed the structure and purity of the ATRP monomer, **M1**. In fact, the key point of the studied synthetic routes relies on the use of inimer **4**, which has mixed functionality: It contains two polymerizable terminal alkenes for ADMET polymerization and one α-bromoisobutyrate group to initiate ATRP and was designed and prepared using a three-step reaction (Scheme 2). The effective formation and purity of **4** were confirmed by ATR–IR (Fig. 2b) and ^{1}H NMR spectroscopies (Fig. 1b).

3.2. Macromonomer synthesis and ADMET polymerization

According to the "Route 1" approach, the macromonomer technique, which was used to synthesize the graft copolymers, forms the basis for our linking ATRP and ADMET polymerization for well-defined graft copolymers possessing narrow molecular weight distributions [24,26]. The controlled radical polymerization of **M1** was first initiated by using inimer **4** as the initiator and CuBr/PMDETA as the catalyst/ligand at 60 °C in THF/CH_3OH. To obtain a macromonomer with a relatively low molecular weight, we initially used a low monomer **M1** to inimer **4** ratio of 15:1. The product was characterized using ^{1}H NMR spectroscopy as shown in Fig. 3a. The structure of the macromonomer was verified through the characteristic resonances of the terminal double bonds at 5.78 (H_r) and 4.96 ppm (H_s) as well as the resonances of the phenyl proton, methylene proton and methyl proton on each **M1** unit at 7.35–7.56 ($H_{h'}$) and 2.12–1.83 ppm (H_x, H_c). By comparing the integration area ratio of phenyl proton from the **M1** unit at 7.35–7.56 ($H_{h'}$, 3H) to that of the terminal alkene proton at 5.78 ppm (H_r, 2H) and including the molecular weight of inimer **4**, the ^{1}H NMR number-average molecular weight ($M_{n,NMR}$ = $[(S_{h'}/3)/(S_r/2)] \times M_{(\mathbf{M1})} + M_{(\mathbf{4})} = 4900$) was determined. The living free-radical conditions of ATRP can be used to generate monodisperse macromonomers before metathesis condensation. The MALLS trace of the macromonomer (Fig. 4) displayed monomodal peaks and a narrow molecular weight distribution of 1.12 with a relatively moderate molecular weight ($M_{n,MALLS}$) of 5100, which

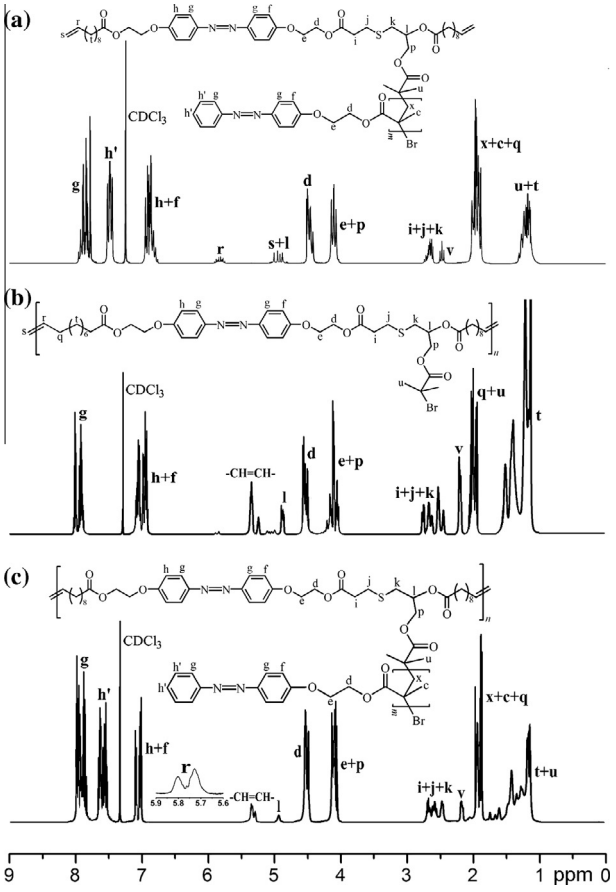

Fig. 3. ^{1}H NMR spectra for the (a) macromonomer, (b) macroinitiator, and (c) graft copolymer.

was found to be close to $M_{n,NMR}$ and the theoretical molecular weight ($M_{n,theo}$ = [**M1**]/[**4**] × yield% × $M_{(\mathbf{M1})}$ + $M_{(\mathbf{2})}$ = 5200).

The diene-containing macromonomer was then converted into a graft copolymer via ADMET polymerization. The metathesis conditions of the macromonomer required high temperatures and extended reaction times [27]. The azo-containing macromonomer was dissolved in toluene, heated to 60 °C, and placed under a slight argon purge to remove ethylene and drive the equilibrium of the polycondensation to completion. ^{1}H NMR technique was used to

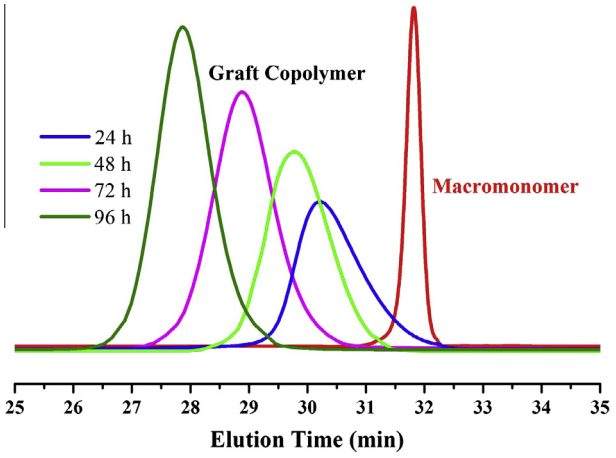

Fig. 4. Representative MALLS–GPC traces for the macromonomer and graft copolymer.

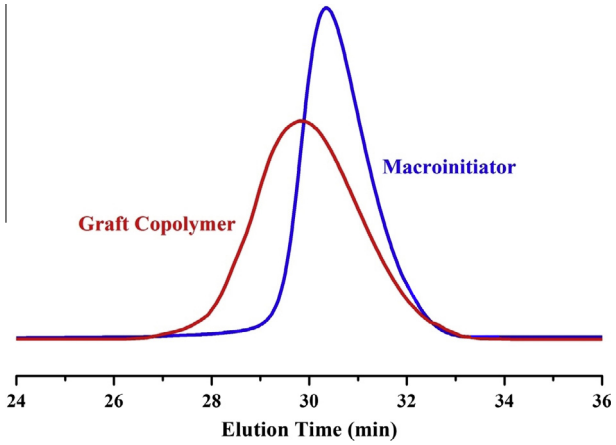

Fig. 5. Representative MALLS–GPC traces for the macroinitiator and graft copolymer.

determine completion of the reaction (Fig. 3c). After extensive reaction times, the resonances of α,ω-diene in macromonomer almost disappeared at 5.78 (H_r) and 4.95 ppm (H_s), whereas the new resonance signal of the internal olefin at 5.43–5.36 ppm was observed. Additionally, all of the other peaks were easily assigned for the macromonomer as well as for the graft copolymer. Then, the number-average molecular weight of the graft copolymer was determined by comparing the integration area ratio of the newly formed internal olefin ($H_{-CH=CH-}$) to that of the terminal alkene (H_r): $M_{n,NMR} = n \times M_{(macromonomer)} - (n-1) \times M_{(ethylene)} = n \times M_{(macromonomer)} - n \times M_{(ethylene)} + M_{(ethylene)} = n \times (M_{(macromonomer)} - M_{(ethylene)}) + M_{(ethylene)} = [(S_{(-CH=CH-)}/2)/(S_r/2)] \times [M_{(macromonomer)}(4900) - M_{(ethylene)}(28)] + M_{(ethylene)}(28)$.

The MALLS curves in Fig. 4 also showed the variation in the molecular weights and molecular weight distributions of the graft copolymers prepared from the macromonomer. We observed that the molecular weights of the resulting copolymers shifted to higher molecular weight positions as the polymerization time increased. The starting macromonomer residue was not observed, indicating that the macromonomer was completely consumed after 24 h, which could be considered positive evidence for the formation of the graft copolymers (Table 1). However, the short lifetime of the catalyst in the reaction solution limited the effectiveness of prolonging the polymerization time for more than 1–2 days, so a fresh batch of 0.5 mol equiv of the catalyst was added to the reaction vessel after 48 h of polymerization [28]. As a result, further growth in the molecular weight of the graft

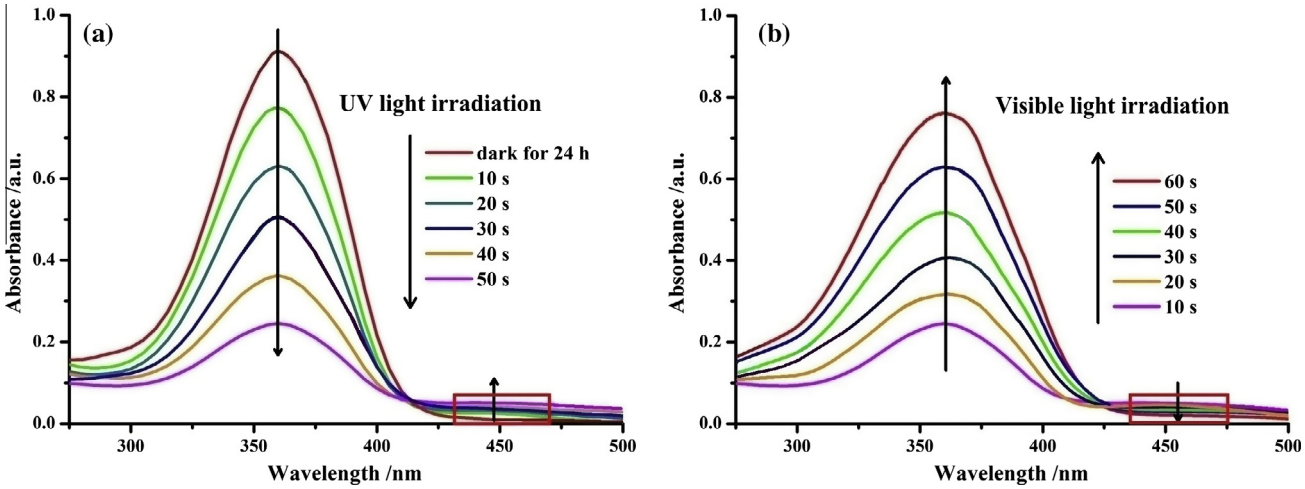

Fig. 6. UV–vis spectral changes as a function of time for a main–chain azo-polymer (macroinitiator) solution in THF with a concentration of 10 mg/mL. (a) Absorbance changes with UV light irradiation (365 nm) and (b) upon irradiating the solution at the photostationary state with visible light.

Table 1
Molecular characteristics of macroinitiator, macromonomer, and graft copolymers as-obtained through "Route 1" and "Route 2" synthetic process.

Polymer	t (h)	Synthetic route	Yield (%)[a]	$M_{n,MALLS}$[b]	M_w/M_n[b]	$M_{n,NMR}$	$DP_{n,backbone}$	$DP_{n,graft}$
Macromonomer	12	ATRP	92	5100	1.07	4900[c]	Nd[g]	13
Macroinitiator	24	ADMET	91	18,300	2.21	17,500[d]	19	Nd
Graft copolymers	24	Route 1	89	26,700	2.23	23,900[e]	5	13
	48		87	50,500	2.08	Nd	10	13
	72		92	89,300	1.89	84,200[e]	18	13
	96		91	127,800	1.92	nd	25	13
	24	Route 2	20	35,500	2.37	36,800[f]	19	3

[a] Obtained gravimetrically from the dried polymer.
[b] Number average molecular weight (M_n) and molecular weight distribution (M_w/M_n) were obtained from multiangle laser light scattering analysis.
[c] Obtained by ^{1}H NMR spectroscopy: $M_{n,NMR} = m \times M_{(M1)} + M_{(inimer)}$, where $m = (S_{h'}/3)/(S_r/2)$, $M_{(M1)} = 310$ and $M_{(inimer)} = 946$.
[d] Obtained by ^{1}H NMR spectroscopy: $M_{n,NMR} = n \times M_{(inimer)} - (n-1) \times M_{(ethylene)}$, where $n = (S_g/4)/(S_r/2)$, $M_{(inimer)} = 946$, and $M_{(ethylene)} = 28$.
[e] Obtained by ^{1}H NMR spectroscopy: $M_{n,NMR} = n \times M_{(Macromonomer)} - (n-1) \times M_{(ethylene)}$, where $n = (S_{-CH=CH-}/2)/(S_r/2)$, $M_{(Macromonomer)} = 4900$, and $M_{(ethylene)} = 28$.
[f] Obtained by ^{1}H NMR spectroscopy: $M_{n,NMR} = m \times M_{(M1)} \times n + M_{(Macroinitiator)}$, where $m = (S_{h'}/3)/(S_{-CH=CH-}/2)$, $M_{(M1)} = 310$, $n = 19$, and $M_{(Macroinitiator)} = 17{,}500$.
[g] Not determined.

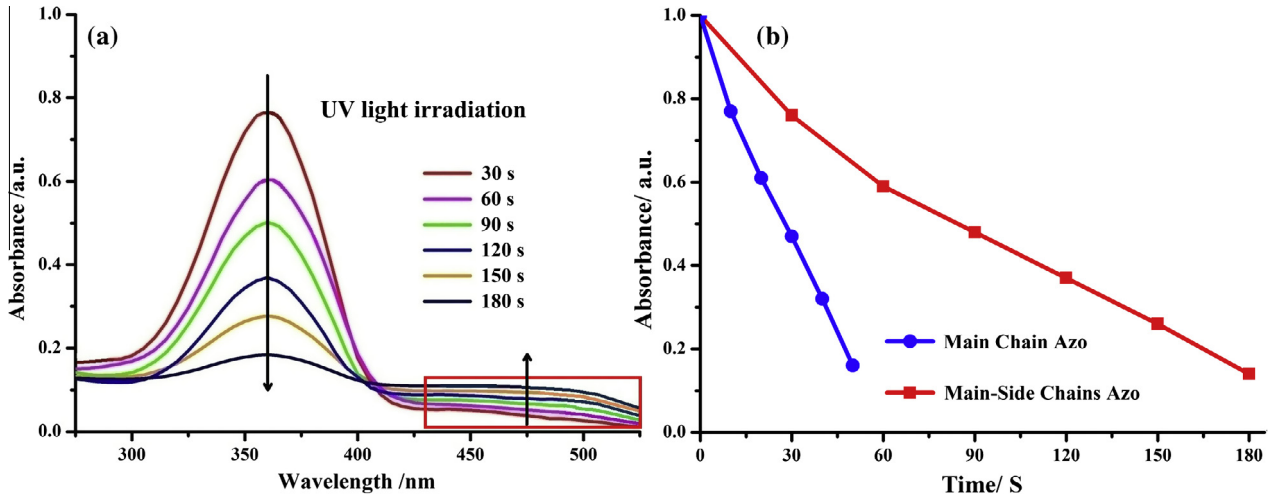

Fig. 7. (a) The photoisomerization of the main–side chain graft azo-copolymer under UV light irradiation (365 nm) and (b) the absorbance of the polymer at 365 nm as a function of irradiation time.

copolymer was detected by MALLS for 72 h and 96 h, as shown in Fig. 4, which was in excellent agreement with the calculated value of $M_{n,NMR}$.

3.3. Macroinitiator synthesis and ATRP

According to "Route 2", the macroinitiator route was also used to synthesize graft copolymers using a multifunctional precursor in which branch growth occurred from multiple initiation sites [24]. The development of the macroinitiator offered several advantages over the macromonomer method. Therefore, ADMET polymerization of inimer **4** was performed first, yielding a higher molecular weight polymer. Then, ADMET polycondensation resulted in macroinitiator for ATRP. However, well-defined graft copolymer structures are typically impossible to synthesize by this technique because it is difficult to initiate every functional site on the macroinitiator. The conversion of the azo-containing α,ω-diene to the internal olefin was closely monitored by ^{1}H NMR spectroscopy (Fig. 3b). As previously noted with the macromonomer, ADMET polymerization occurred. The successful polymerization was indicated by reductions in the intensities of the peaks at 5.78 and 4.95 ppm and an increase in the peak at 5.43–5.36 ppm. Analogously, the number-average molecular weight of the macroinitiator could be determined using the end group analysis process ($M_{n,NMR} = n \times M_{(\mathbf{4})} - (n-1) \times M_{(ethylene)}$, $n = (S_g/4)/(S_r/2)$). The MALLS trace in Fig. 5 shows a relatively moderate molecular weight distribution ($M_w/M_n = 2.21$) and high molecular weight ($M_{n,MALLS} = 17{,}500$), which was in agreement with $M_{n,NMR}$ (Table 1).

The obtained azo-functionalized ADMET polymer bearing many initiating sites could be employed as a macroinitiator in subsequent ATRP of **M1** to synthesize graft copolymers with azo side chains. A homogeneous reaction mixture was retained throughout the entire reaction process, even when the viscosity of the mixture increased as the polymerization progressed. The combination of ADMET polymerization and ATRP following the route depicted in "Route 2" yielded a graft copolymer, as shown by MALLS–GPC (Fig. 5), where a clear-cut shift in the copolymer trace toward lower retention volumes (with respect to the macroinitiator) was observed while the molecular weight distribution became slightly more broad (Table 1). The growth of **M1** graft chains was also indicated by ^{1}H NMR, and the molecular weight agreed with the MALLS data. However, these data correlated with a **M1** chain of approximately 3 repeat units per initiation site. These results did not agree with the calculated values of 15 repeat units of **M1** and indicated that the initiation did not occur quantitatively, i.e., ATRP had lost some efficiency in this system.

3.4. Photoresponsive behavior in solution

Polymers containing azo-type chromophores have *cis* and *trans* isomers. Generally, the *cis* form of the azo molecule is thermodynamically less stable than the *trans* form. Therefore, when there is a lack of visible light, the *cis* form, which is obtained by photoisomerization, will change into the *trans* form. We first investigated the photoresponsive properties of the representative main-chain azo-polymer in solution. As illustrated by the UV–vis spectra in Fig. 6, the macroinitiator THF solution was exposed to varying conditions of UV or visible light irradiation, which underwent the *trans* to *cis* photoisomerization (Fig. 6a) and the *cis* to *trans* back-isomerization process (Fig. 6b). Then, we characterized the UV isomerization efficiency of the azo-polymer by calculating the ratio of $A^{trans-cis}/A_0$, which denoted the absorbance at the photostationary state of the UV-induced *trans* to *cis* isomerization process [29]. A_0 is the absorbance maximum of the sample after 24 h in the dark. For the main-chain azo-polymer, the photoisomerization efficiency was 0.88, which indicated that most of the azo groups underwent the isomerization process.

In this case, there are two types of azo groups in the main and side chains of the photosensitive graft copolymer; thus, the isomerization process of the chromophore will be very complicated [30,31]. UV–vis spectroscopy was used to characterize the complicated photoisomerization process of the azo moieties. It showed a strong absorption at 364 nm, which is attributed to the $\pi \rightarrow \pi^*$ transition in the *trans* isomer, and a wide absorption peak at 456 nm, which is attributed to the $n \rightarrow \pi^*$ transition in the *cis* isomer. We also observed a shoulder peak at 495 nm, which might be due to the absorbance of *cis–trans*, *trans–cis* or *cis–cis* isomers. With increasing irradiation time, the absorbance of these two peaks increased at similar rates (Fig. 7a). This result indicated that *cis* isomers increasingly appeared. However, when the main or side azo groups isomerized, the quantity of *cis* and *trans* isomers should be equal in the *cis–trans* and *trans–cis* isomers. The shoulder peak at 495 nm must be due to the absorption of *cis–trans* and/or *trans–cis* isomers but not *cis–cis* isomers. If this peak originated from *cis–cis* isomers, the absorbance at 364 nm should disappear because there are no single *trans* azo groups remaining. After 60 s of irradiation, the shoulder peak disappeared and merged into a broad peak between 450 and 525 nm, indicating complete photochemical

conversion from the *trans–trans* isomer configuration to the *cis–cis* isomer configuration and the existence of a photostationary state. Furthermore, Fig. 7b shows that the photoisomerization rates of the azo functional macroinitiator (main chain) and graft copolymer (main–side chains) showed the same trend as the photoisomerization percentages. The macroinitiator gave a higher isomerization rate, while the graft copolymer gave a lower one. This result suggested that one type of azo group had a faster photoisomerization rate than the two types under UV irradiation, which agreed with the possible photoisomerization mechanism of main–side-on azo chromophores.

4. Conclusion

Well-defined graft copolymers containing azo units in all of the main and side chains were successfully synthesized via the combination of living ATRP and ADMET chemistry. Compared with typical macroinitiator syntheses of graft copolymers (Route 2), the macromonomer synthetic approach (Route 1) allowed for precise control of the architecture. Upon irradiation with UV or visible light, the photoisomerization process of the azo chromophores were monitored by the UV–vis spectra. We found that the isomerization of the azo groups in the main and side chains occurred mainly on one type of azo group, and the main–side-on structure resulted in the two types of azo groups having similar isomerization probabilities. These results suggested that the azo chromophore percentage was decisive in the photoisomerization rate of the chromophores and the main–side-on structure of the azo chromophores favored the photoisomerization.

Acknowledgments

The authors thank the National Natural Science Foundation of China (No. 21304079) and the Initial Scientific Research Foundation of Yancheng Institute of Technology (KJC2014002) for financial support of this research.

References

[1] A. Natansohn, P. Rochon, Chem. Rev. 102 (2002) 4139–4176.
[2] (a) A. Shishido, Polym. J. 42 (2010) 525–533;
(b) A. Priimagi, C.J. Barrett, A. Shishido, J. Mater. Chem. C 2 (2014) 7155–7162.
[3] T. Seki, S. Nagano, M. Hara, Polymer 54 (2013) 6053–6266.
[4] H.F. Yu, J. Mater. Chem. C 2 (2014) 3047–3054.
[5] X.Q. Xue, J. Zhu, Z.B. Zhang, N.C. Zhou, Y.F. Tu, X.L. Zhu, Macromolecules 43 (2010) 2704–2712.
[6] C. Ohm, M. Brehmer, R. Zentel, Adv. Mater. 22 (2010) 3366–3387.
[7] (a) Y.N. He, X.G. Wang, Q.X. Zhou, Polymer 43 (2002) 7325–7333;
(b) P.C. Che, Y.N. He, X.G. Wang, Macromolecules 38 (2005) 8657–8663.
[8] (a) X.Q. Xue, J. Zhu, Z.B. Zhang, N.C. Zhou, X.L. Zhu, React. Funct. Polym. 70 (2010) 456–462;
(b) Y.N. Zhang, X. Zhu, N.C. Zhou, X.R. Chen, W. Zhang, Y.G. Yang, X.L. Zhu, Chem. Asian J. 7 (2012) 2217–2221.
[9] T. Yoshino, M. Kondo, J. Mamiya, M. Kinoshita, Y. Yu, T. Ikeda, Adv. Mater. 22 (2010) 1361–1363.
[10] X.Y. Jiang, X.B. Chen, X.G. Yue, J.J. Zhang, S.W. Guan, H.B. Zhang, W.Y. Zhang, Q.D. Chen, React. Funct. Polym. 70 (2010) 616–621.
[11] B. Yameen, A. Farrukh, Chem. Asian J. 8 (2013) 1736–1753.
[12] S.S. Sheiko, M. Moller, Chem. Rev. 101 (2001) 4099–4124.
[13] S.S. Sheiko, B.S. Sumerlin, K. Matyjaszewski, Prog. Polym. Sci. 33 (2008) 759–785.
[14] H. Jiang, F.J. Xu, Chem. Soc. Rev. 42 (2013) 3394–3426.
[15] W.V. Camp, V. Germonpré, L. Mespouille, P. Dubois, E.J. Goethals, F.E.D. Prez, React. Funct. Polym. 67 (2007) 1168–1180.
[16] (a) C. Cheng, E. Khoshdel, K.L. Wooley, Macromolecules 40 (2007) 2289–2292;
(b) M.R. Xie, J.Y. Dang, H.J. Han, W.Z. Wang, J.W. Liu, X.H. He, Y.Q. Zhang, Macromolecules 41 (2008) 9004–9010.
[17] H.C. Shi, D. Shi, L.G. Yin, S.F. Luan, J. Zhao, J.H. Yin, React. Funct. Polym. 70 (2010) 449–455.
[18] (a) P. Seven, M. Coşkun, K. Demirelli, React. Funct. Polym. 68 (2008) 922–930;
(b) M. Coskun, P. Seven, React. Funct. Polym. 71 (2011) 395–401.
[19] L. Ding, J. Qiu, J. Wei, Z.S. Zhu, Macromol. Rapid Commun. 35 (2014) 1509–1515.
[20] K.L. Opper, K.B. Wagener, J. Polym. Sci., Part A: Polym. Chem. 49 (2011) 821–831.
[21] P. Atallah, K.B. Wagener, M.D. Schulz, Macromolecules 46 (2013) 4735–4741.
[22] M.D. Schulz, R.R. Ford, K.B. Wagener, Polym. Chem. 4 (2013) 3656–3658.
[23] H. Mutlu, L. Montero de Espinosa, M.A.R. Meier, Chem. Soc. Rev. 40 (2011) 1404–1445.
[24] (a) P.M. O'Donnell, K.B. Wagener, J. Polym. Sci., Part A: Polym. Chem. 41 (2003) 2816–2827;
(b) D. Markova, K.L. Opper, M. Wagner, M. Klapper, K.B. Wagener, K. Müllen, Polym. Chem. 4 (2013) 1351–1363.
[25] (a) L. Ding, L.Y. Zhang, H.J. Han, W. Huang, C.M. Song, M.R. Xie, Y.Q. Zhang, Macromolecules 42 (2009) 5036–5042;
(b) L. Ding, G.D. Yang, M.R. Xie, D.Y. Gao, J.H. Yu, Y.Q. Zhang, Polymer 53 (2012) 333–341;
(c) L. Ding, M.Y. Xu, J.J. Wang, Y. Liao, J. Qiu, Polymer 55 (2014) 1681–1687.
[26] (a) K. Matyjaszewski, M. Teodorescu, P.J. Miller, M.L. Peterson, J. Polym. Sci., Part A: Polym. Chem. 38 (2000) 2440–2448;
(b) H. Shinoda, P.J. Miller, K. Matyjaszewski, Macromolecules 34 (2001) 3186–3194;
(c) H. Shinoda, K. Matyjaszewski, Macromolecules 34 (2001) 6243–6248.
[27] J.E. Schwendeman, A.C. Church, K.B. Wagener, Adv. Synth. Catal. 344 (2002) 597–613.
[28] I.A. Gorodetskaya, T.-L. Choi, R.H. Grubbs, J. Am. Chem. Soc. 129 (2007) 12672–12673.
[29] X.Q. Shen, H.W. Liu, Y.S. Li, S.Y. Liu, Macromolecules 41 (2008) 2421–2425.
[30] M. Jin, R. Lu, Q.X. Yang, C.Y. Bao, R. Sheng, T.H. Xu, Y.Y. Zhao, J. Polym. Sci., Part A: Polym. Chem. 45 (2007) 3460–3472.
[31] J.J. Zhang, H.B. Zhang, X.B. Chen, J.H. Pang, Y.X. Zhang, Y.P. Wang, Q.D. Chen, S.H. Pei, W.X. Peng, Z.H. Jiang, React. Funct. Polym. 71 (2011) 553–560.